IDENTIFYING CLIMATE CHANGE VULNERABILITY BASED ON LAND COVER INDICATORS: A CASE STUDY IN SURABAYA, INDONESIA

Floriberta BINARTI [1]* , ***Albertus Joko SANTOSO*** [2]

DOI : 10.21163/GT_2023.181.06

ABSTRACT :
Surabaya is facing the threat of climate change indicated by the increase in air and surface temperature. The city has a risk of sinking by 2050 if the global warming cannot be resolved. Several related studies established that the change in land cover and land use is accompanied by the increase in surface temperature, which will be addressed in this present study. Therefore, this study aimed to examine the impact of land use/cover on the increase in air/surface temperature and investigate the contribution of land cover indicators to climate change in Surabaya as the basis of the identification of spatial climate change vulnerability. Data were collected from satellite images obtained over a long period and processed with GIS-based software to obtain an overview of changes. Mined long-term historical climate data and satellite imagery were processed into a land surface temperature map (LST), describing the tendency of climate change. The satellite imagery data from 2013 to 2021 was used to have an overview of land use and land cover changes based on indicators of built-up area (NDBI), surface imperviousness (NDISI), vegetation (NDVI), and water (NDWI). The contribution of each indicator to the surface temperature was analyzed using the multivariate regression method. The significant contribution of the land cover indicators to the surface temperature as the results means that NDBI, NDISI, NDVI, and NDWI can be used as indicators in climate change vulnerability assessment. The sequential contribution weights to the surface temperature are NDISI, NDWI, NDVI, and NDBI. Furthermore, the climate change vulnerability map of Surabaya City was developed based on the contribution weights, which the pattern of vulnerability levels corresponds to the pattern of water index values.

Key-words: *Climate change vulnerability, Land cover indicator, Satellite imagery, Surface temperature.*

1. INTRODUCTION

The occurrence of climate change is marked by an increase in global surface temperature of 0.86ºC from 2006 to 2015, accompanied by frequent hot airwaves and an increase in the frequency and intensity of rainfall (IPCC, 2019). The 2015 Paris Climate Agreement requires countries to limit global warming to 1.5ºC by 2050 due to its increased risks to health, livelihoods, food security, and water supplies (IPCC, 2021). The Meteorology, Climatology, and Geophysics Agency results from 1960 to 2021 showed an increase in air temperature in Indonesia from 0.8 to 1.4 ºC (BMKG, 2022). Aside from the temperature rise, global warming is also indicated by the increase in sea level, whereby Jakarta, Surabaya, and other capital cities in the northern coast of Java are predicted to sink in 2050, as stated in Climate Central (2022).

According to the International Panel on Climate Change, the adverse impact risk of climate change depends on the hazard, exposure, and vulnerability (Allen et al., 2018). In the context of climate change, vulnerability is the degree to which a system is amenable to the hostile impacts of climate change, including climate variability and extremes. (IPCC, 2007; Gumel, 2022). A system is considered vulnerable when it is exposed and shows sensitivity to climatic changes with low adaptive capacity. Hence, assessment of vulnerability to climate change is very important to identify hot spots

[1] *Department of Architecture, Universitas Atma Jaya Yogyakarta, Jl. Babarsari 44 Sleman 55281, Indonesia, floriberta.binarti@uajy.ac.id. Corresponding author**

[2] *Department of Informatics, Universitas Atma Jaya Yogyakarta, Jl. Babarsari 44 Sleman 55281, Indonesia, joko.santoso@uajy.ac.id*

of climate change that require urgent attention to lessen the climate change impacts for sustainable development (Schneiderbauer et al., 2020).

Identifying the right indicators for each component of the vulnerability function is an important step in the development process of climate change vulnerability assessment methodologies. Many studies identified the assessment indicators from the perspective of the disaster impacts of climate change (Ludena et al., 2015; Nguyen et al., 2016; Schneiderbauer et al., 2020; UN-Habitat, 2019), while only a few did from the potential causes (Delaney et al., 2021). United Nations Habitat manual, for example, developed the current disaster risk profile (risk index) to map the most vulnerable areas. The indicators for measuring vulnerability are exposure to hazards, ecosystem, socio-economic, and infrastructure components (UN-Habitat, 2019). The objective of disaster impact-based assessment indicators is to define the degree of adaptive capacity and further propose an effective adaptation method to climate change. To achieve the goal of sustainable development, however, climate-resilient trajectories should combine adaptation and mitigation (Denton et al., 2014). The goal of mitigation is to alleviate the exposure and reduce the vulnerability to climate change (IPCC, 2007). Potential causes-based assessment indicators aim to formulate effective mitigation strategies. For mapping the climate change vulnerability of aquatic-riparian ecosystems, Delaney et al. (2021) chose some exposure indicators classified into hydrology, precipitation, and temperature. Whether disaster impact- or potential cause-based indicators, the assessment method should be guided by five principles – i.e., simplicity, measurability and availability of data, inclusiveness, comprehensiveness, and spatial relevance (Ludena et al., 2015).

To identify climate change vulnerability at a local scale (a city), an understanding of climate change issues at a national scale could help to figure out the major causes. Schneiderbauer et al. (2020) showed the urgency of a vulnerability assessment at a national scale before identifying local-specific drivers of vulnerability and appropriate adaptation measures. According to the 2020 ND-GAIN Country Index, Indonesia is identified as vulnerable to climate change impacts with the rank of 97nd out of 181 countries. Indonesia is exposed highly to flooding (ranked 17th most at risk from this natural hazard) and tropical cyclones (ranked 23rd). High maximum temperatures with an average monthly maximum of around 30.6ºC occur regularly (World Bank & ADB, 2021). It was reported that a significant proportion of the greenhouse gas (GHG) emissions in Indonesia emanate from land use change, which represented 52.3% of total GHG emissions in Indonesia between 2000 to 2017 (World Bank & ADB, 2021). At the global scale, a review of 116 studies on the role of land use and land cover change in climate change vulnerability assessments conducted by (Santos et al., 2021) mentioned that 34% of the studies assumed climate change and land use/cover change would act addictively, while 66% allowed for interactive effects. Moreover, land use/cover is an environmental factor, which is one of the four internal vulnerability factors mentioned by the United Nations (2014) (Esperón-Rodríguez et al., 2016), that relevant to reduce the disaster.

Two questions arise regarding indicators of climate change vulnerability for Surabaya – i.e., (1) Does land use/cover determine climate change indicated by the temperature increase? (2) Can land cover indicators be used to assess climate change vulnerability? (3) How much does the contribution of each land cover index to climate change? Therefore, this study was conducted to answer the questions based on the following objectives:

(1) To examine the impact of land use/cover in Surabaya on climate change;
(2) To investigate the contribution of each land cover indicator to climate change in Surabaya City;
(3) To develop a climate change vulnerability map of Surabaya to support decision-makers in prioritizing the implementation of climate change mitigation strategies.

2. STUDY AREA

The study area is situated in Surabaya City, East Java, Indonesia (**Fig. 1**). As the second largest city in Indonesia, the population in Surabaya increased yearly. According to the Central Bureau of Statistics of East Java record, at the beginning of 2019, the registered population was 3,095,026 people, increasing by about 0.52% from 2010 to 2017 (BPS Jawa Timur, 2018). JICA stated that the land in Surabaya is used for agriculture (1.6%), non-irrigation agriculture (0.03%), settlements (39%),

ponds (11.4%), water (2.2%), industry (8.5%), green areas and recreation (8.5%), public facilities (7.1%), forests, mangrove forests and swamps (5.8%), and commercial areas (4.6%); while the remaining (8.3%) are vacant (Savitri et al., 2019). A study using remote sensing data from 1996 to 2015 revealed the land use change from mangrove forest into pond land. The pond area changed from 673 ha in 1996 to 3,139.66 ha in 2015 (Savitri et al., 2019).

There were 23 events consisting of tornadoes, drought, forest and land fires, and floods in 2008-2017 reported by Surabaya City Disaster Risk Assessment Document for 2019-2023. During this period, Surabaya experienced whirlwinds (7 events), drought (2 events), forest and land fires (1 event), and flooding (Kurniawati et al., 2020). Kurniati & Nitivattananon (2016) stated that the growth trend towards East Surabaya raises urban heat island (UHI) – the city experiences much warmer temperature than the surrounding rural areas - in Surabaya with a temperature difference of ±1.4ºC, while Jatayu & Susetyo (2017) mentioned that a 6.62ºC rise between 2001 and 2016. According to Syafitri et al. (2020), the UHI deviation of ±1.59ºC in East Surabaya is correlated with changes in land use, building density, and sky view factor. However, Pratiwi & Jaelani (2020) illustrated the fluctuation of the surface temperature from the processing of satellite imagery showing that the average surface temperature in 2002, 2014, and 2019 was 29.09ºC, 26.89ºC, and 27.13ºC, respectively.

Fig. 1. Location of Surabaya City on the map of South East Asia (source: Google Map).

3. DATA AND METHODS

3.1. Data sources

The rise of global air/surface temperature change indicates global warming that causes climate change. Historical air temperature data can be obtained from weather stations. However, the data has low accuracy in reflecting regional temperatures and lack appropriate spatial resolution. Surface temperature data sourced from satellite imagery can provide precise information on spatially ground surface temperatures (Firozjaei et al., 2018). Moreover, remote sensing provides end-users with a consistent, repeatable, and relatively inexpensive methodology for land surface temperature, land cover, and vegetation mapping (Azevedo et al., 2016). However, the weakness of satellite images compared to climate data from weather stations is their availability on specific dates with an accuracy level determined by the cloud cover. In many previous studies, GIS-based software was used to classify satellite images to determine the effect of changes and indicators in land use/cover on the climate surface temperature of cities (Majeed et al., 2021; Maleki et al., 2020).

This study used air and surface temperature data from mining climate data from the nearest weather stations and processing Landsat 8 OLI/TIRS imagery over 10 years obtained from Earth Explorer (https://earthexplorer.usgs.gov/). Satellite imagery is also used to produce maps of land cover indicators. Landsat can detect surface temperatures with a higher resolution than other images with thermal channels because it is equipped with 60 m and 100 m resolution infrared channels (Fawzi, 2017). Furthermore, satellite images of Surabaya City were taken at the latitude of 7.32° S and longitude of 112.71° E with a 20 km radius using images with less than 10% cloud cover.

The land use land cover change (LULCC) analysis provides an overview of the locations and areas experiencing land use/cover changes by comparing two satellite images acquired in different years. To determine the changes in land use/cover, this study downloaded the MODIS Land Cover v.6 satellite image for Surabaya from 2013 to 2021 in Earth Explorer. However, the images can be replaced by Landsat 8 OLI/TIRS B4, B5, and B6 images. By using a qGIS feature, LULC analysis comparing two images in specific years can show changes in surface temperature. **Table 1** presents the data sources used in this study.

Table 1.

Data sources.

The kind of data	Date/year	Source/method	Usage
Historical air temperature data	2013-2021	Data mining	To observe the trend of air temperature increases
Landsat 8 OLI/TIRS	2013-2021	USGS - Earth Explorer https://earthexplorer.usgs.gov/	To observe the land cover changes
MODIS Land Cover v.6	2013-2021	USGS - Earth Explorer https://earthexplorer.usgs.gov/	To analyze the land use land cover change

Only less than ten images of the 33 satellite images of Surabaya City obtained from 2013 to 2021 can produce maps without cloud cover. Four dates of retrieved satellite imagery were presented to illustrate the change in temperature surface and land cover indicators. **Table 2** describes the cloud cover, time, and sun elevation data collected for satellite imagery. It shows that the four satellite images were taken at almost the same hour with little sun elevation.

Table 2.

Date, cloud cover, hour, and sun elevation of the satellite images.

Date	Cloud cover	Hour	Sun Elevation
13/08/2013	6.82	02:37:46	54.13
20/09/2015	3.41	02:35:43	62.35
28/09/2018	0.83	02:35:28	63.85
01/10/2019	9.39	02:36:07	64.43

3.2. Classification of satellite image data

We used land cover indicators to observe the land cover change. Yang and Chen (2016) stated that green plot ratio, built-up ratio, impervious surface fraction, and surface admittance are land cover indicators that can be obtained from satellite image processing. The extraction of Landsat 8 OLI/TIRS imagery consisting of nine spectral bands can be used to classify the land cover indicators. Green plot ratios can be generated from normalized difference vegetation index (NDVI) maps. Built-up ratios can be described by normalized difference built-up index (NDBI) maps. Meanwhile, the impervious surface fraction was generated from normalized difference impervious surface index (NDISI) maps. Normalized difference water index (NDWI) was used to describe the surface admittance. Values of LST and the land cover indicators were calculated using the equation explained in the following sub-sub sections. Meanwhile, the analysis of LULCC utilized semi-automatic classification in qGIS, an open source GIS software (Majeed et al., 2021). Furthermore, maps of the LST and land cover indices were classified using the K-Nearest Neighbors (KNN) method. KNN is an ML algorithm widely used to classify land cover indicators from satellite imagery (Binarti et al., 2021; Ge et al., 2020; Jiang et al., 2020).

3.2.1. Land Surface Temperature (LST)

LST maps (in ^{o}C) were obtained by rasterizing satellite images and clustering using Eq. (1)–(5) (Jeevalakshmi et al., 2017).

$$LST = \frac{BT}{\left\{1+\lambda*\left(\frac{BT}{p}\right)*ln(LSE)\right\}} \quad [^{o}C] \tag{1}$$

$$BT = \frac{K2}{\ln\left(\frac{K1}{L}+1\right)} - 272.15 \quad [^{o}C] \tag{2}$$

$$LSE = (0.004 * Pv) + 0.986 \tag{3}$$

$$Pv = \left\{{}^{(NDVI - NDVImin)}/_{NDVImax - NDVImin}\right\}^2 \tag{4}$$

$$NDVI = \frac{(NIR-RED)}{(NIR+RED)} \tag{5}$$

where:

BT	-brightness temperature;
λ	-average wavelength of band 10;
p	-the multiplying of Planck's constant by Boltzmann constant and velocity of light (14380);
K1 and K2	-band-specific thermal conversion constant;
L	-spectral radiance;
LSE	-land surface emissivity;
Pv	-the proportion of vegetation;
NDVI	-normalized difference vegetation index;
NIR	-near-infrared band;
RED	-red band

3.2.2. Normalized Difference Built-up Index (NDBI)

NDBI in satellite imagery is the ratio map of the built-up to the total area. Xu et al. (2018) developed Eq. (6) using NIR and short-wavelength infrared band (SWIR) as variables.

$$NDBI = \frac{(SWIR-NIR)}{(SWIR+NIR)} \tag{6}$$

3.2.3. Normalized Difference Imperviousness Surface Index (NDISI)

Xu (2010) developed Eq. (7) to determine the relationship between the thermal band (TIR), the near-infrared band (NIR), the middle infrared band (MIR), and the visible band (VIS) on impervious surfaces based on satellite imagery.

$$NDISI = \frac{\left\{TIR - \frac{1}{3} * (VIS + NIR + MIR)\right\}}{\left\{TIR + \frac{1}{3} * (VIS + NIR + MIR)\right\}} \quad (7)$$

3.2.4. Normalized Difference Vegetation Index (NDVI)

Towers et al. (2019) tested NDVI's ability to estimate spatial variability and found that it is more accurate than other vegetation indices. The NDVI value is extracted using Eq. (5).

3.2.5. Normalized Difference Water Index (NDWI)

NDWI estimates water bodies' area, depth, and turbidity (Mcfeeters, 2007). Meanwhile, Eq. (8) is a modification of the basic formula sensitive to changes in the water content in the leaves (Gao, 1996).

$$NDWI = \frac{(NIR - SWIR)}{(NIR + SWIR)} \quad (8)$$

NDWI=(NIR-SWIR)/(NIR+SWIR)

Where SWIR is the short wavelength infrared band (1.24 μ m) value.

3.3. Accuracy assessment

Since surface temperature is the most important variable in identifying the spatial climate change vulnerability index based on land cover indicators, we compared the surface temperature of three points measured using infra-red camera FLIR i5 to the surface temperature of the same locations at the same time resulted from satellite image processing. The infra-red camera FLIR i5 has a thermal sensitivity of less than 0.1ºC and the capability to measure temperatures ranging from -20°C to 250°C with a resolution of 0.1°C. Since there is only one package of satellite image data, which is free of cloud and available during climate monitoring (from August 12 to September 12, 2022), we compared the measured surface temperatures to the ones on the LST map on August 12, 2022, 02:48:18.

3.4. Data analysis

Multivariate regression analysis with a 95% confidence level was used to analyze the effect or contribution of each land cover index - i.e., NDBI, NDISI, NDVI, and NDWI - as independent variables and the surface temperature (LST) as the dependent variable. The reliability and validity of the variables were determined by the coefficient (R-squared) and the p-value. R-squared describes the percentage of the response variable. When the p-value is less than the significance level (0.05), the sample data provide sufficient evidence to reject the null hypothesis for the entire population (Andrade, 2019). Furthermore, Beta Coefficient was used to describe the effect strength of each independent variable on the dependent.

4. RESULTS

4.1. Accuracy of land surface temperature calculations.

Table 3 describes the comparison between measured surface temperatures and surface temperatures in the LST map on August 12, 2022, 02:48:18. The surface temperature differences of points 1, 2, and 3 are only 0.54%, 0.03%, and 0.15% respectively.

Table 3.

Results of the accuracy assessment of LST calculations.

Point	Geographical location	Surface temperature		
		Measured (ºC)	Satellite image (ºC)	Difference (ºC)
1	7º46'01"S & 110º24'24"E	33.6	33.42	0.18
2	7º46'52"S & 110º25'24"E	33.0	32.99	0.01
3	7º46'56"S & 110º23'30"E	33.3	33.25	0.05

4.2. Temperature increases and the land cover profile

The temperature increases are described by the air temperature trend (**Fig. 2**) and LST maps (**Fig. 3**). **Fig. 2** illustrates the trend of increasing the maximum, average, and minimum air temperature obtained from mining nine-year climate data for Surabaya from 2013 to 2021. Despite the insignificant increases, the average air temperature rose from less than 27ºC to slightly more than 27ºC. The air temperature trends show that the greatest increase sequentially was experienced by the maximum air temperatures. The maximum air temperature in 2013 was less than 31ºC and in 2021 reached almost 32ºC.

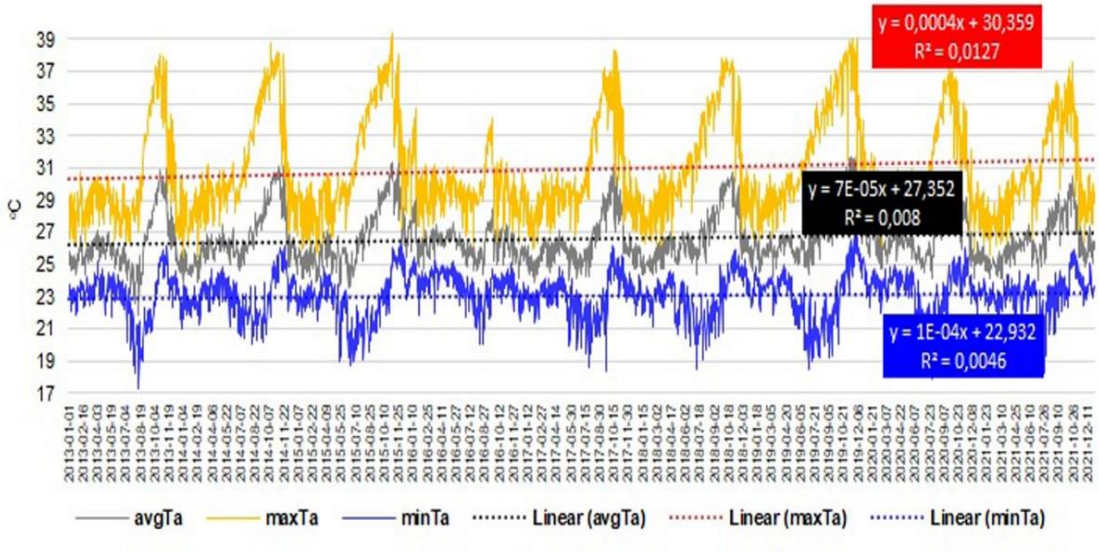

Fig. 2. Trend of temperature increases in Surabaya in 2013-2021.

The LST map was also used to observe climate change on four representative dates from 2013 to 2019, namely 08/13/2013, 20/09/2015, 28/09/2018, and 01/10/2019. **Fig. 3** illustrates the minimum and average increase in surface temperature in 2015 from 29.19ºC to 29.41ºC and 32.79ºC to 32.86ºC, respectively. In 2018 the minimum and average surface temperatures decreased to 29.28ºC and 32.41ºC, respectively. However, in 2019, the minimum and average surface temperatures were 29.71ºC and 33.05ºC. Although the maximum surface temperature increased in 2018 and 2019, the maximum surface temperature in 2019 at 36.50ºC was lower than in 2013 (i.e., 36.75ºC). The illustration of the surface temperature fluctuation confirms the results of the study by Pratiwi & Jaelani (2020). Maps of land cover indicators in **Fig. 3** show remarkable changes in the water index (NDWI). From 2013 to 2019, the maximum, average, and minimum water index experienced a gradual decrease from -0.43 to -1.07, 0.06 to -0.11, and 0.77 to 0.51, respectively. A significant increase appears in the maximum value of the built-up index (NDBI) – i.e., from 0.77 in 2013 to 0.84 in 2019. The vegetation index (NDVI) decreased in the minimum and maximum values. However, the average water index increased from 0.15 in 2013 to 0.25 in 2019. A significant increase in the impervious surface index (NDISI) only occurred in the maximum value from 0.71 in 2013 to 0.80 in 2019. The average value increased insignificantly from 0.62 in 2013 to 0.63 in 2019.

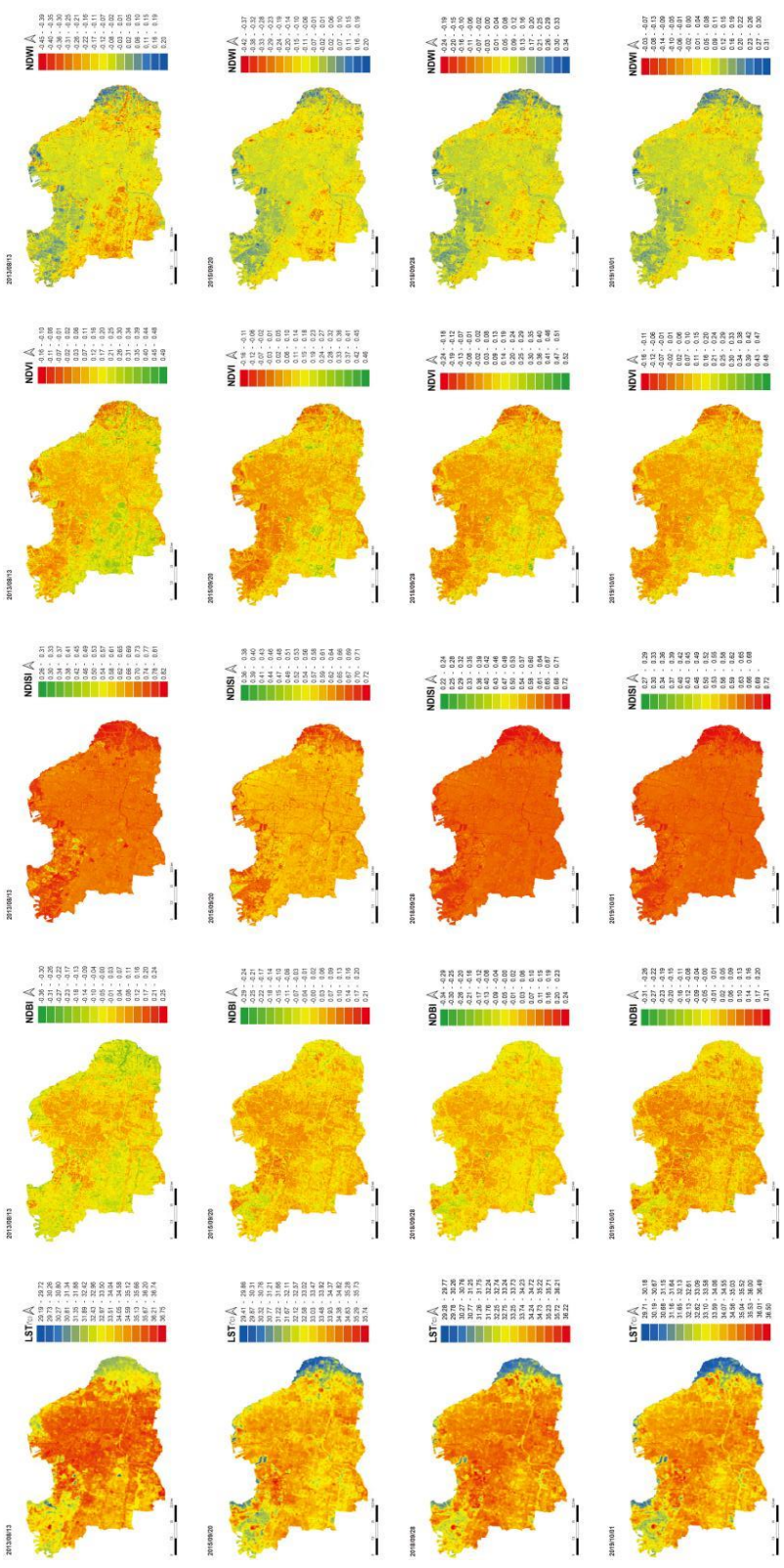

Fig. 3. Map of LST, NDBI, NDISI, NDVI, NDWI Surabaya City on 13/08/2013, 20/09/2015, 28/09/2018, and 01/10/2019

4.3. Land use land cover change (LULCC)

Fig. 4 presents two comparisons between two land cover/use images in 2013 (the duration beginning) and 2015 (the first surface temperature increase) and between two land cover/use images in 2015 and 2019 (the last surface temperature increase). The map of LULCC in 2013 and 2015 shows that the built area dominates Surabaya by 41.3%. Conversely, the map of LULCC in 2015 and 2019 was dominated by changes in agricultural land to the built-up areas by 32.6%. However, the percentage of the total built-up area between 2015 and 2019 was 64%, which is the cumulative of the built-up area without change (26.6%), change of water body (3.3%), green area (1.5%), and agricultural land. The percentage of built-up area in 2019 was much larger than in 2015 (43.3%). The most significant land use change between 2013 and 2015 was from green areas to agricultural land (8.6%), followed by changes from built-up areas to agricultural land (8.2%).

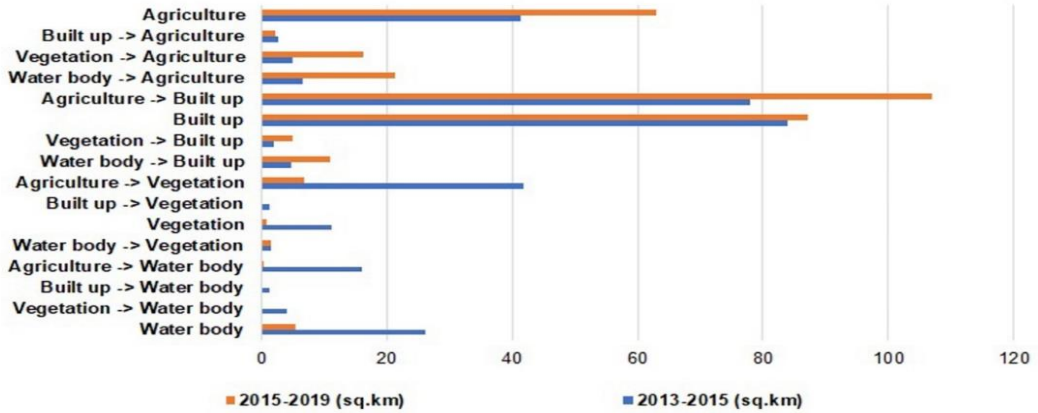

Fig. 4. The land use/land cover change histogram of Surabaya City.

Changes from water body to other functions, which covered 10% of the total area in 2019 and 16% of the total area including the reduction of the water body area from 2015 to 2019, appeared dominantly in **Fig. 5**. The land use changes are detected in the north, northwest, and southeast areas of Surabaya. These maps also depict the change/reduction of vegetation and agriculture to the built-up area found in the southwest and southeast of the study area. This change/reduction consumed 37% of the total area. The increase in a built-up area is only 1% of the total area. Positive land use change (from built-up into vegetation area) only occurred in 2013-2015, which is only 0.44% of the total area. Although some areas in 2015-2019 experienced a change from water bodies into agriculture/vegetation areas prominently as shown in **Fig. 5 (right)**, however, the areas displayed in the 01/10/2019 NDWI map in **Fig. 3** still have high water index values.

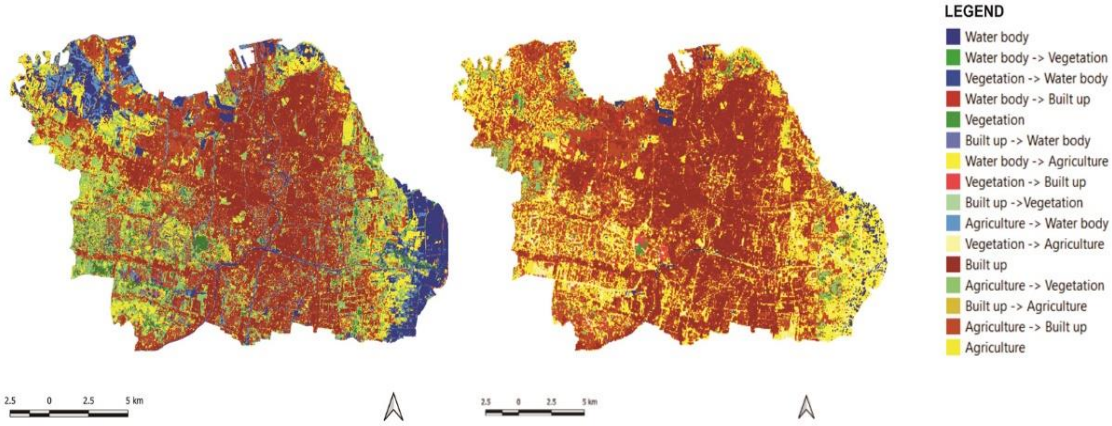

Fig. 5. The land use/land cover change map of Surabaya City: 2013 – 2015 (left) and 2015 – 2019 (right).

4.4. Contribution of each land cover index

The multivariate regression analysis of the contribution of each land cover indicator to land surface temperature was conducted in the latest satellite image data aiming to determine high-level vulnerability areas for the current implementation of climate change mitigations. The results of multivariate regression of five satellite image dates show that satellite imagery of October 1, 2019, has the highest R-squared, as shown in **Table 4**. The R-squared of 0.85 is considered high, which explains that the four land cover indicators on October 1, 2019, affected 85% of surface temperature. Therefore, the contribution weights of four land cover indices were used to develop a climate change vulnerability map. Less than 0.05 of the p-value for all variables indicates that the four land cover indicators determine the surface temperature. Based on the Beta Coefficient of each land cover index, it can be concluded that NDISI has the largest contribution, followed by NDWI and NDVI. This order of contributions also applies to the other four satellite images of the dates.

Table 4.

Coefficient of determination (R-squared) and P-value.

Date	R-squared	β coefficient				P-value			
		NDBI	NDISI	NDVI	NDWI	NDBI	NDISI	NDVI	NDWI
June 26, 2018	0.78	0.19	14.93	-1.40	-1.51	0.00	0.00	0.00	0.00
June 11, 2019	0.81	0.00	17.12	-1.57	-3.26	0.00	0.00	0.00	0.00
July 29, 2019	0.76	0.76	10.48	-3.04	-3.38	0.00	0.00	0.00	0.00
October 01, 2019	0.85	1.13	9.83	-5.33	-5.69	0.00	0.00	0.00	0.00

4.5. Climate change vulnerability map

Based on the contribution weights from the multivariate regression analysis of satellite imagery data obtained on October 1, 2019, we developed the climate change vulnerability (see **Fig. 6**) using an equation derived from the contribution weights – i.e., Vulnerability Level = (9.83*NDISI) - (5.69*NDWI) - (5.33*NDVI) + (0.85*NDBI) – in **Table 4**. The orange and red areas indicate a high-level of vulnerability to climate change. The red areas randomly scattered in the southwest, west, north, east, and southeast must be prioritized firstly for climate change mitigation.

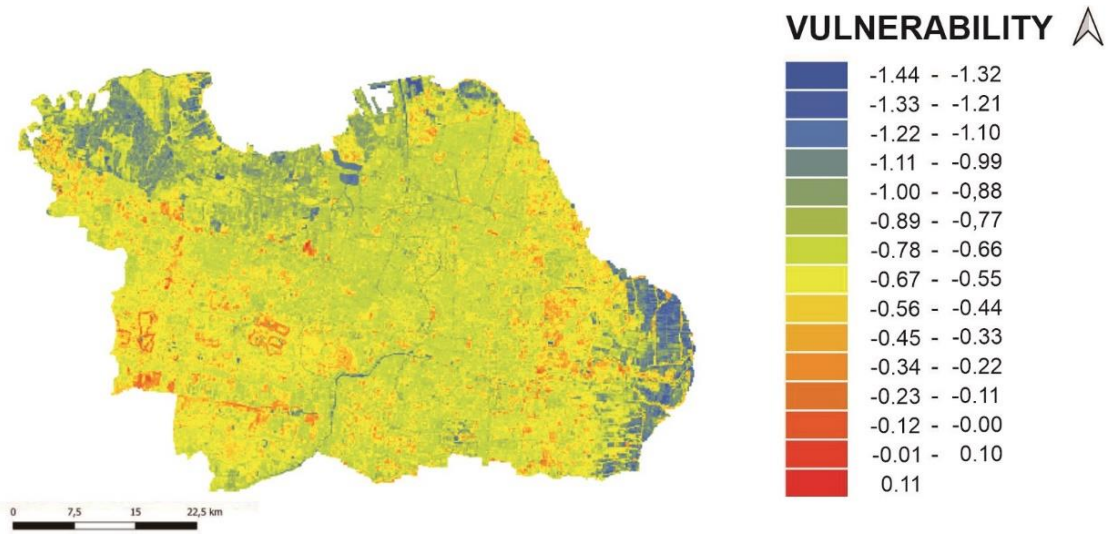

Fig. 6. The climate change vulnerability map of Surabaya City.

5. DISCUSSION

The increase in air and surface temperature during the last nine years indicates climate change in Surabaya. Approximately 1ºC of the increase in average air temperature in Surabaya already exceeds the recently observed global warming trends of 0.2ºC per decade (IPCC, 2019). Moreover, any increase in global temperature (+0.5ºC) was projected to affect human health negatively and heat-related morbidity and mortality (Hoegh-Guldberg et al., 2018).

The trend of air temperature increase in **Fig. 2** corresponds to the gradual reduction in minimum, average, and maximum values of the water index and the increase in the maximum value of the built-up index. The similar pattern of the water index, built-up index, and surface temperature in **Fig. 3** confirms the effect of water index reduction on the (surface) temperature. The highest surface temperature areas located in the center and southern Surabaya are related to the areas with the lowest water index and highest built-up index. An increase in surface temperature can be observed in the east area of Surabaya adjacent to ponds and swamps from 2013 to 2015. Changes from non-built areas (such as water bodies) to built-up areas in the eastern part also appeared on the NDBI and NDWI maps in 2013-2015. The change from a green to a built-up area emerged in the southwest area on the NDBI and NDVI maps. However, the change in surface temperature on the southwest side did not appear prominently on LST maps

Fig. 3 and **Fig. 5** demonstrated that changes in the maximum surface temperature are related to land use changes. The increase in maximum values of the built-up index was in line with the dominance of built-up areas without changes in **Fig. 4**. **Fig. 5 (left)** shows those changing from other land use in 2013-2015 located in the city's center, north and south sides of Surabaya. In 2015-2019, however, the development of built-up areas appeared towards the northwest and east shown in **Fig. 5 (right)**. The percentage of the total area that has changed from a built-up to agricultural land (0.65%), agricultural land to a green area (5.8%), built-up area to a green area (5.2%), and agricultural area to a water body (4.5%). This is in line with the decrease in maximum surface temperature in 2013 and 2015 as shown in **Fig. 4**. Surabaya's urban park development program is one of the causes of this positive change in land use and cover. Setiawati et al. (2021) reported that from 1995 to 2016 the bare land in the southwestern and central part of Surabaya was converted into green parks. Furthermore, the increase in minimum, average, and maximum surface temperatures in 2015 and 2019 is in line with the percentage of land use change into built-up areas (64%) supported by changes in water bodies and green areas to agricultural land at 6.5% and 4.9%, respectively. The change in water bodies into agricultural land obviously can be observed in eastern Surabaya.

Although the impervious surface index contributed most to land surface temperature, the NDISI and LST maps did not reveal similar patterns. Maps of NDWI and NDBI that own similar patterns with LST maps became the second and fourth contributors. However, when the contribution weights were applied to the vulnerability map, the pattern of vulnerability level corresponded to the pattern of the water index values in NDWI maps. Areas with high water index values are the least vulnerable, and vice versa. The study on the relationship between water index and surface temperature on various land surfaces in India (Guha & Govil, 2021) also describes the strong correlation between water index and surface temperature, especially during the post-monsoon season.

Since the correlation between surface temperature and land cover indices could change following the season (Guha & Govil, 2021), future studies on the seasonal impact of land cover indices on the surface temperature would corroborate the contribution weights and develop a more reliable climate change vulnerability map. To use satellite images acquired in every season, more images with higher cloud cover should be included. Consequently, cloud removal in the preprocessing step must be done to lower the risk of loss of information leading to a spatiotemporal discontinuity that degrades the quality and usefulness of satellite images (Hasan et al., 2022).

6. CONCLUSIONS

As one of the cities on the northern coast of Java has a risk of sinking by 2050, Surabaya needs an urgent formulation of climate change adaptation and mitigations. Moreover, an increase in air temperature, as shown by nine-year historical climate data, confirms the occurrence of global warming as an indication of climate change. Since land use/cover change became the significant cause of climate change in Indonesia, land cover indicators can be used as the base for identifying climate change vulnerability. Some findings regarding the trend of air temperature increase, land surface temperature (LST), and four land cover indicators – i.e., built-up index (NDBI), impervious surface index (NDISI), vegetation index (NDVI), and water index (NDWI) – describe the specific characteristic of land use/cover in Surabaya and the impact of land cover on the increase in air and surface temperature. The trend of air temperature increases is in line with the values of the water and built-up index, which are presented in the NDWI and NDBI maps, respectively.

The LULCC maps illustrate the change of water areas mainly to agriculture and built-up areas. However, the multivariate regression analysis results explained the significant contribution of land cover indicators to the surface temperature. Sequentially, land cover indicators that contribute to the surface temperature of Surabaya are the index of surface imperviousness (NDISI), water body/content (NDWI), vegetation (NDVI), and built-up (NDBI). The climate change vulnerability map of Surabaya City developed based on the contribution weight shows the pattern of vulnerability levels corresponding to the water index values in NDWI maps. Future studies on the projected climate change vulnerability map by 2050 will be needed to achieve global warming of less than 1.5ºC.

REFERENCES

Allen, N.M. et al. (2018) Framing and Context. In: Global Warming of 1.5ºC. An IPCC Special Report on the impacts of global warming of 1.5ºC above pre-industrial levels and related global greenhouse gas emission pathways, in the context of strengthening the global response, In press. IPCC.

Andrade, C. (2019) The P Value and Statistical Significance: Misunderstandings, Explanations, Challenges, and Alternatives. *Indian J Psychol Med.*, 41(3), 210‑215.

Azevedo J.A., Chapman L. & Muller C. L. (2016) Quantifying the Daytime and Night-Time Urban Heat Island in Birmingham, UK: A Comparison of Satellite-Derived Land Surface Temperature and High Resolution Air Temperature Observations. *Remote Sensing*, 8, 153.A.

Binarti, F., Triyadi, S., Koerniawan, M.D., Pranowo, P. & Matzarakis, A. (2021) Climate characteristics and the adaptation level to formulate mitigation strategies for a climate-resilient archaeological park. Urban Climate, 36, 100811.

BMKG (Badan Meteorologi Klimatologi dan Geofisika) (2022) Ekstrem Perubahan Iklim. BMKG. URL: https://www.bmkg.go.id/iklim/?p=ekstrem-perubahan-iklim.

BPS (Badan Pusat Statistik) Provinsi Jawa Timur (2018) Jumlah Penduduk dan Laju Pertumbuhan Penduduk Menurut Kabupaten/Kota di Provinsi Jawa Timur 2010, 2016 dan 2017. BPS Jawa Timur.

Climate Central (2014) Coastal Risk Screening Tool: Land Projected to be Below Annual Flood Level in 2050. URL: https://coastal.climatecentral.org/map/12/123.9254/10.3001/?theme=sea_level_rise&map_type=coastal_dem_comparison&contiguous=true&elevation_model=coastal_dem&forecast_year=2050&pathway=rcp45&percentile=p50&return_level=return_level_1&slr_model=kopp_2014.

Delaney, J.T, Bouska, K.L., Eash, J.D., Heglund, P.J., Allstadt, A.J. (2021) Mapping climate change vulnerability of aquatic-riparian ecosystems using decision-relevant indicators. *Ecological Indicators*, 125, 107581.

Denton, F., Abeysinghe, A.C., Burton, I., Gao, Q., Lemos, M.C., Masui, T., O'Brien, K.L. & Warner, K. (2014) Climate-resilient pathways: adaptation, mitigation, and sustainable development. In: Field, C.B., Barros, V.R., Dokken, D.J., Mach, K.J., Mastrandrea, M.D., Bilir, T.E., White, L.L (Eds.), *Climate Change 2014: Impacts, Adaptation, and Vulnerability. Part A: Global and Sectoral Aspects. Contribution of Working Group II to the Fifth Assessment Report of the Intergovernmental Panel on Climate Change*. Cambridge University Press, Cambridge, 1101‑1131.

Esperón-Rodríguez, M., Bonifacio-Bautista, M., Barradas, V.L. (2016) Socio-economic vulnerability to climate change in the central mountainous region of eastern Mexico. *Ambio*, Mar 45(2), 146-60.

Fawzi, N.I. (2017) Mengukur urban heat island menggunakan penginderaan jauh, kasus di Kota Yogyakarta. *Majalah Ilmiah Globe*, 19, (2), 195.

Firozjaei, M.K., Kiavarz, M., Alavipanah, S.K., Lakes, T. & Qureshi, S. (2018) Monitoring and forecasting heat island intensity through multi-temporal image analysis and cellular automata-Markov chain modelling: a case of Babol City, Iran. *Ecological Indicators*, 91, 155‑170.

Gao, B. (1996) NDWI A Normalized Difference Water Index for Remote Sensing of Vegetation Liquid Water From Space. *Remote Sensing Environment*, 58, 257‑266.

Ge, G., Shi, Z., Zhu, Y., Yang, X. & Hao, Y. (2020) Land use/cover classification in an arid desert-oasis mosaic landscape of China using remote sensed imagery: Performance assessment of four machine learning algorithms. *Global Ecology and Conservation*, 22, e00971.

Guha, S. & Govil, H. (2021) Relationship between land surface temperature and normalized difference water index on various land surfaces: A seasonal analysis. *International Journal of Engineering and Geosciences*, 6(3), 165-173.

Gumel, D.Y. (2022) Assessing Climate Change Vulnerability: A Conceptual and Theoretical Review. *Journal of Sustainability and Environmental Management (JOSEM)*, 1(1), 22 ‑ 31.

Hasan, C., Horne, R., Mauw, S. & Mizera, A. (2022) Cloud removal from satellite imagery using multispectral edge-filtered conditional generative adversarial networks. *International Journal of Remote Sensing*, 43(5), 1881-1893.

Hoegh-Guldberg, O., Jacob, D., Taylor, M., Bindi, M., Brown, S., Camilloni, I., Diedhiou, A., Djalante, R., Ebi, K.L., Engelbrecht, F., Guiot, J., Hijioka, Y., Mehrotra, S., Payne, A., Seneviratne, S.I., Thomas, A., Warren, R. & Zhou, G. (2018) Impacts of 1.5°C Global Warming on Natural and Human Systems. In: Global Warming of 1.5° C. An IPCC Special Report on the impacts of global warming of 1.5ºC above pre-industrial levels and related global greenhouse gas emission pathways, in the context of strengthening the global response to the threat of climate change, sustainable development, and efforts to eradicate poverty. Cambridge University Press, Cambridge, UK and New York, NY, USA, 175-312.

IPCC (Intergovernmental Panel on Climate Change) (2007) Climate change 2007: Synthesis report. In: *Contribution of Working Groups I, II and III to the Fourth Assessment Report of Environmental Panel on Climate Change, IPCC*. Switzerland, IPCC, Geneva.

IPCC (2019) Global Warming of 1.5ºC. An IPCC Special Report on the impacts of global warming of 1.5ºC above pre-industrial levels and related global greenhouse gas emission pathways, in the context of strengthening the global response to the threat of climate change, sustainable development, and efforts to eradicate poverty. IPCC Working Group I Technical Support Unit.

IPCC (2021) Projected Climate Change, Potential Impacts and Associated Risks. URL: https://www.ipcc.ch/sr15/resources/headline-statements/.

Jatayu, A. & Susetyo, C. (2017) , Analisis Perubahan Temperatur Permukaan Wilayah Surabaya Timur Tahun 2001-2016 Menggunakan Citra LANDSAT. *Jurnal Teknik ITS*, 6(2), C429-C433.

Jeevalakshmi, D., Reddy, S.N. & Manikiam, B. (2017) Land Surface Temperature Retrieval from LANDSAT data using Emissivity Estimation. *International Journal of Applied Engineering Research*, 12(20), 9679-9687.

Jiang, F., Smith, A.R., Kutia, M., Wang, G., Liu, H. & Sun, H. (2020) A modified kNN method for mapping the leaf area index in arid and semi-arid areas of China. *Remote Sensing*, 12, 1‑24.

Kurniati, A.C. & Nitivattananon, V. (2016) Factors influencing urban heat island in Surabaya, Indonesia. *Sustainable Cities and Society*, 27, 99-105.

Kurniawati, U.F., Susetyo, C. & Setyasa, P.T. (2020) Institutional assesment through climate and disaster resilience initiative in Surabaya. *IOP Conference Series: Earth Environmental Science*, 562, 012025.

Ludena, C.E., Yoon, S.W., Sánchez-Aragón, L., Miller, S. & Yu, B-K. (2015) *Vulnerability Indicators of Adaptation to Climate Change and Policy Implications for Investment Projects*. Inter-American Development Bank, Technical Note No. 858, Washington DC.

Majeed, M., Tariq, A., Anwar, M.M., Khan, A.M., Arshad, F., Mumtaz, F., Farhan, M., Zhang, L., Zafar, A., Aziz, M., Abbasi, S., Rahman, G., Hussain, S., Waheed, M., Fatima, K. & Shaukat, S. (2021) Monitoring of Land Use‑Land Cover Change and Potential Causal Factors of Climate Change in Jhelum District, Punjab, Pakistan, through GIS and Multi-Temporal Satellite Data. *Land*, 10, 1026.

Maleki, M., Van Genderen, J.L., Tavakkoli-Sabour, S.M., Saleh, S.S. & Babaee, E. (2020) Land use/cover change in Dinevar rural area of West Iran during 2000-2018 and its prediction for 2024 and 2030. *Geographia Technica*, 15 (2), 93-105.

Mcfeeters, S.K., 2007. The use of the Normalized Difference Water Index (NDWI) in the delineation of open water features. *International Journal of Remote Sensing*, 17, 1425‑1432.

Nguyen, T.T.X., Bonetti, J., Rogers, K. & Woodroffe, C.D. (2016). Indicator-based assessment of climate-change impacts on coasts: a review of concepts, methodological approaches and vulnerability indices. *Ocean and Coastal Management*, 123, 18-43.

Pratiwi, A.Y. & Jaelani, L.M. (2020) Analisis Perubahan Distribusi Urban Heat Island (UHI) di Kota Surabaya Menggunakan Citra Satelit Landsat Multitemporal. *Jurnal Teknik ITS*, 9(2), C48-C55.

Pratiwi, A.Y. & Jaelani, L.M. (2020) Analisis Perubahan Distribusi Urban Heat Island (UHI) di Kota Surabaya Menggunakan Citra Satelit Landsat Multitemporal. *Jurnal Teknik ITS*, 9(2), C48-C54.

Safitri D.A., Bespalova L.A., Wijayanti F. (2019) Changes in land use in Eastern Surabaya, Indonesia, and their impact on coastal society and aquaculture. *R-economy*, 5(4), 198‑207.

Santos, M.J., Smith, A.B., Dekker, S.C., Eppinga, M.B., Leita˜o, P.J., Moreno-Mateos, D., Morueta-Holme, N. & Ruggeri, M. (2021) The role of land use and land cover change in climate change vulnerability assessments of biodiversity: a systematic review. *Landscape Ecology*, 36, 3367‑3382.

Schneiderbauer, S., Baunach, D., Pedoth, L., Renner, K., Fritzsche, K., Bollin, C., Pregnolato, M., Zebisch, M., Liersch, S., López, M.R.R. & Ruzima, S. (2020) Spatial-Explicit Climate Change Vulnerability Assessments Based on Impact Chains. Findings from a Case Study in Burundi. *Sustainability*, 12, 6354.

Setiawati, M.D., Jarzebski, M.P., Gomez-Garcia, M. & Fukushi, K. (2021) Accelerating Urban Heating Under Land-Cover and Climate Change Scenarios in Indonesia: Application of the Universal Thermal Climate Index. *Frontier in Built Environment*, 7, 622382.

Syafitri, R.A.W.D., Pamungkas, A. & Santoso, E.B. (2020) The Impact of Urban Configuration to the Urban Heat Island in East Surabaya. *IPTEK Journal of Proceeding Series*, 6, 470-477.

Towers, P.C., Strever, A. & Poblete-echeverr, C. (2019) Comparison of Vegetation Indices for Leaf Area Index Estimation in Vertical Shoot Positioned Vine Canopies with and without Grenbiule Hail-Protection Netting. *Remote Sensing*, 11, 1073.

UN Habitat (2019) Climate Change Vulnerability Assessment Manual. United Nations (UN) Habitat, URL: https://unhabitat.org/climate-change-vulnerability-assessment-manual

World Bank and ADB (Asian Development Bank) (2021) Climate Risk Country Profile: Indonesia. World Bank and ADB Report, Washington.

Xu, H. (2010) Analysis of Impervious Surface and its Impact on Urban Heat Environment using the Normalized Difference Impervious Surface Index (NDISI). *Photogrammetric Engineering and Remote Sensing*, 76, 557‑565.

Xu, R., Liu, J. & Xu, J. (2018) Extraction of high-precision urban impervious surfaces from sentinel-2 multispectral imagery via modified linear spectral mixture analysis. *Sensors* (Switzerland) 18, 1‑15.

Yang, F. & Chen, L. (2016) Developing a thermal atlas for climate- responsive urban design based on empirical modeling and urban morphological analysis. *Energy and Building*, 111, 120‑130.